

See discussions, stats, and author profiles for this publication at: <https://www.researchgate.net/publication/276208361>

Sequence-Dependent Solvation Dynamics of Minor-Groove Bound Ligand Inside Duplex-DNA

ARTICLE *in* THE JOURNAL OF PHYSICAL CHEMISTRY B · MAY 2015

Impact Factor: 3.3 · DOI: 10.1021/acs.jpcb.5b01977 · Source: PubMed

CITATION

1

READS

35

4 AUTHORS, INCLUDING:



Sachin Dev Verma

University of South Carolina

8 PUBLICATIONS 76 CITATIONS

[SEE PROFILE](#)



Nibedita Pal

Bowling Green State University

7 PUBLICATIONS 83 CITATIONS

[SEE PROFILE](#)



Sobhan Sen

Jawaharlal Nehru University

36 PUBLICATIONS 993 CITATIONS

[SEE PROFILE](#)

Sequence-Dependent Solvation Dynamics of Minor-Groove Bound Ligand Inside Duplex-DNA

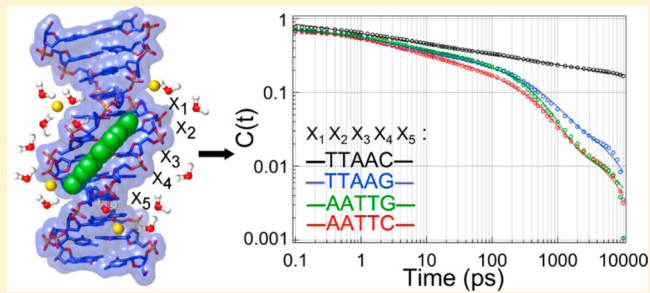
Sachin Dev Verma, Nibedita Pal, Moirangthem Kiran Singh, and Sobhan Sen*

Spectroscopy Laboratory, School of Physical Sciences, Jawaharlal Nehru University, New Delhi 110067, India

Supporting Information

ABSTRACT: Ligand binding to minor-grooves of DNA depends on DNA-base sequence near its binding-site. However, it is not known how base-sequences affect the local solvation of ligand inside minor-grooves of DNA. Here we present a comprehensive study on sequence-dependent solvation dynamics of ligand inside duplex-DNA by measuring the static and dynamic fluorescence Stokes shifts of a popular groove-binder, DAPI, inside DNA minor-grooves created by four different sequences; $d(5'-CGCGAATTGCGC-3')_2$, $d(5'-CGCGTTAACGCG-3')_2$, $d(5'-CGCGCAATTGCGC-3')_2$, and $d(5'-CGCGCTTAAGCGC-3')_2$, having different sequences near DAPI-binding site.

Fluorescence up-conversion and time-correlated single photon counting techniques are employed to capture the dynamic Stokes shifts of DAPI over five decades in time from 100 fs to 10 ns. We show that the ligands sense different static and dynamic solvation inside minor-grooves created by different sequences: Only subtle change in the dynamics is seen in DNA containing -AATTG-, -TTAAC-, and -AATTC- sequences, which show power-law relaxation in initial time-decades, followed by biexponential decay in nanosecond time-scales. However, changing a single base (and the complementary base) near ligand-binding site from -TTAAC- to -TTAAC- drastically induces the dynamics to follow a single power-law relaxation over the entire five decades. The observed variation of dynamics possibly relate to the local DNA motions, coupled to the hydration dynamics near the ligand-binding site.



INTRODUCTION

Synthetic cationic small molecules (ligands) bind to DNA, showing useful therapeutic effect against various diseases.^{1–3} While direct electrostatic and van der Waals interactions between (cationic) ligands and (anionic) DNA facilitate the ligand–DNA complex formation, specific hydrogen bonding and rearrangements of water and ions near the complex are also found to play important role in stabilizing ligands inside DNA.^{4–9} Ligand binding to DNA-grooves are found to displace water and ions from the grooves, leading to favorable entropic contribution to the binding energy.^{4–9} Such desolvation and ion expulsion is also found in the case of protein binding to DNA.^{10,11} In fact, dynamics of water release/uptake is shown to play a vital role in controlling the solvation free energy of drug–DNA interactions.¹² Hence, understanding the dynamics of local solvation around ligands inside DNA is crucial for elucidating the complex interactions of drugs with DNA.

Sequence-dependent groove-widths and their dynamics inside DNA are vital for various proteins to readout the DNA-sequences.^{13–17} A large database on DNA–protein complexes unfolds that the electrostatic potentials of DNA minor-grooves are modulated by the sequence-dependent groove geometry, which can be elegantly recognized by proteins.¹⁸ Similar to proteins, ligand binding to DNA also depend on base-sequence of DNA near the binding site.^{19–24} Minor grooves with AT-rich sequences are found to be

narrower compared to GC-rich sequences, which are easily recognized by most of the groove-binding ligands with high affinities ($\sim 10^7$ – 10^8 M⁻¹).^{4,6,19–21,25–29} The complementary shapes (isohelicity) of AT-rich minor-grooves and ligands are believed to be the key factors that govern such tight binding,^{3,25,30} although the binding of linear-shaped ligands to minor-grooves suggests that isohelicity is not the only factor that facilitates ligand binding, but formation of strong hydrogen bonds between ligand and DNA as well as local hydration structure promote such interactions.^{4,31} More importantly, ligands are found to bind with different affinities and conformations to minor grooves created by different AT-/TA-rich sequences.¹⁹ Not only that, X-ray^{20,27} and MD simulation²¹ studies showed that changing a single base (and the complementary base) near the AT-region can actually alter the binding site of ligands inside minor-grooves of DNA. Change in groove widths upon ligand binding is also reported.³² Nevertheless, despite availability of a large sum of structural information, what is not known is how the local dynamics solvate ligands inside minor-grooves of DNA created by different AT-/TA-rich sequences.

Special Issue: Biman Bagchi Festschrift

Received: February 28, 2015

Revised: April 19, 2015

Published: May 12, 2015

This article tackles these issues by measuring the dynamic Stokes shifts over five decades in time from 100 fs to 10 ns of a well-known DNA-binding ligand, DAPI (4',6-diamidino-2-phenylindole), inside minor-grooves of DNA created by four different AT-/TA-rich sequences. By monitoring the DAPI fluorescence and its time evaluation, we are able to show that DAPI binds differently to the minor-grooves created by different base-sequences and sense different dynamics of solvation. Results are implicative that the local solvation structure and dynamics around ligands inside minor-grooves are depended on the base-sequence and local DNA motions, possibly coupled to the motions of nearby water molecules.

Time-resolved fluorescence Stokes shift (TRFSS) and related experiments have the capability to measure solvation dynamics around a probe inside biomolecules directly on the time-scales of collective motions of water, ions, and biomolecule.^{33–35} TRFSS has been widely used to study solvation dynamics in simple water,³⁶ ionic liquids,^{37,38} proteins,^{39,40} DNA,^{5,41–50} protein–DNA complexes,^{51–53} supramolecular assemblies,⁵⁴ and even biological cells.^{55,56} TRFSS experiments measure the dynamics of solvation by recording the time-dependent change of electrostatic interaction energy of a probe (here DAPI) with its surrounding charged/dipolar molecules (i.e., water, ions, and DNA).³⁶ The charge distribution inside probe changes upon optical excitation. Subsequently, surrounding molecules reorient by exerting reaction electric field to stabilize the excited charge distribution inside the probe. This leads to the shifting of fluorescence spectra of the probe toward lower energies, which in turn reports the dynamics of solvation around the probe in solution.³⁶

DAPI is a popular fluorescent marker for DNA, which has various applications.⁵⁷ DAPI is useful as antiparasitic, antiviral, and anticancer drugs⁵⁸ and is also found to play an important role in inhibiting the action of RNA polymerase II by blocking the TATA-box binding protein to bind DNA.^{59,60} DAPI is extensively used as fluorescent marker in biochemical and cytochemical studies, including fluorescence imaging.⁶¹ An important property of DAPI (and also of other groove-binding ligands) is that it has very low fluorescence quantum yield in bulk water, but its fluorescence gets enhanced by many folds upon binding to DNA.⁶² DAPI is shown to preferentially bind to minor grooves of DNA having AT-rich sequences.^{6,19–21} It has been also shown that the binding affinity of DAPI changes drastically if the AT-rich sequence is reversed to TA-rich sequence near its binding site.¹⁹ The binding affinity is actually found to decrease with base-sequence as AATT \gg TAAT \approx ATAT $>$ TATA \approx TTAA.¹⁹ However, X-ray crystallographic study showed that change in the base flanking to AATT sequence has remarkable effect on the binding site of DAPI.²⁰ It has been found that DAPI binds near the central AATT region of –AATTC– sequence. However, changing the flanking base from ‘C’ to ‘G’ shifts the DAPI binding-site by one base toward ATTG.²⁰ Recent MD simulations support such finding.²¹ Similar effect is also seen for other minor groove binder, Hoechst.²⁷ Nevertheless, the question remains is how ligand solvation occurs inside such minor grooves of DNA created by different central sequences having different flanking bases.

Here we study the static and dynamic solvation around DAPI inside minor grooves of duplex-DNA formed by four different (central) sequences: $d(5'-\text{CGCG}\underline{\text{AATT}}\text{CGCG}-3')_2$, $d(5'-\text{CGCG}\underline{\text{TTAAC}}\text{CGCG}-3')_2$, $d(5'-\text{CGCG}\underline{\text{CAATT}}\text{CGCG}-3')_2$, and $d(5'-\text{CGCG}\underline{\text{CTTAAAG}}\text{CGCG}-3')_2$ in the presence of Na^+ ions. The choice of ligand and base-sequences is made based on

the following criteria: (1) Size of DAPI is smaller compared to other fluorescent minor-groove binders,⁴ which shall occupy smaller space near its binding-site. Hence, we expect to see maximum variation in its local static and dynamic solvation when bound inside minor-grooves of different sequences. (2) Duplex-DNA having AT-steps is known to be narrower and rigid, while DNA with TA-steps is wider and flexible.^{63–65} These sequences possess different local dynamics at base-level, which are coupled to the local hydration water inside minor-grooves.⁶⁶ Hence, we may be able to capture the maximum variation in dynamics due to change in groove-widths as well as the local DNA-motion coupled to hydration dynamics. (3) Changing the base flanking to central four-bases from ‘C’ to ‘G’ shifts the DAPI binding site toward the flanking ‘G’.^{20,21} Hence, we would be able to observe the effect of single base change in solvation of the ligand. We also expect that if the ligand displaces different amounts of water and ions from the grooves formed by the different sequences, or if the sequence-dependent change in groove-widths modulate the number of water and ions near the ligand-binding site then we will be able to capture the different collective motions of water, ions, and DNA-proper as sensed by the ligand inside minor-grooves of different sequences. Fluorescence up-conversion (UPC) and time-correlated single photon counting (TCSPC) techniques are employed to measure the TRFSS of DAPI in DNA over five decades in time from 100 fs to 10 ns. We found only subtle but distinguishable difference in dynamics in the case of –AATTG–, –TTAAG–, and –AATTC–, where the dynamics follow power-law until \sim 100 ps, followed by biexponential decay that equilibrate rapidly near 10 ns. However, severe sequence dependence is observed in replacing a single base (and the complementary base) from –TTAAG– to –TTAAC–, which induces the dynamics to follow a single power-law relaxation over the entire five decades from \sim 100 fs to 10 ns.

MATERIALS AND METHODS

DAPI (4',6-diamidino-2-phenylindole, dilactate; Figure 1A) was from Sigma-Aldrich, used without further purification. Desalted and HPLC-purified self-complementary single-stranded oligonucleotides of 14-mer, 5'-CGCGCAATTG-CGCG-3' and 5'-CGCGCTTAAAGCGCG-3', and 12-mer, 5'-CGCGAATTCGCG-3' and 5'-CGCGTTAACCGCG-3' were also from Sigma-Aldrich. Duplex-DNA were prepared by resuspending single-stranded oligonucleotides in 100 mM sodium phosphate buffer of pH 7, and by annealing strands from 95 °C to room temperature (25 °C) over \sim 5 h (\sim 14 min/°C). The formation of double-stranded B-form DNA was confirmed by measuring the circular dichroism (CD) spectra of the samples using CD spectrometer (ChriScan, Applied Photophysics), which show characteristic negative peak near \sim 255 nm (see Figure S1 in Supporting Information). All samples were prepared in HPLC grade water (Merck). The concentrations of DNA-duplexes were measured by UV-visible absorption spectrophotometer (Shimadzu, model-UV2450) at 260 nm using duplex extinction coefficients of 220 366 M^{–1} cm^{–1} (–AATTG–), 221 417 M^{–1} cm^{–1} (–TTAAG–), 191 511 M^{–1} cm^{–1} (–AATTC–), and 192 203 M^{–1} cm^{–1} (–TTAAC–), calculated from nearest-neighbor model.^{67,68} (Note that throughout the article we will omit writing the bases preceding and following the central five-bases and will denote the sequences as –XXXXX–.) All experiments were performed with concentration ratio of [DAPI]/[DNA] = 1:5, where

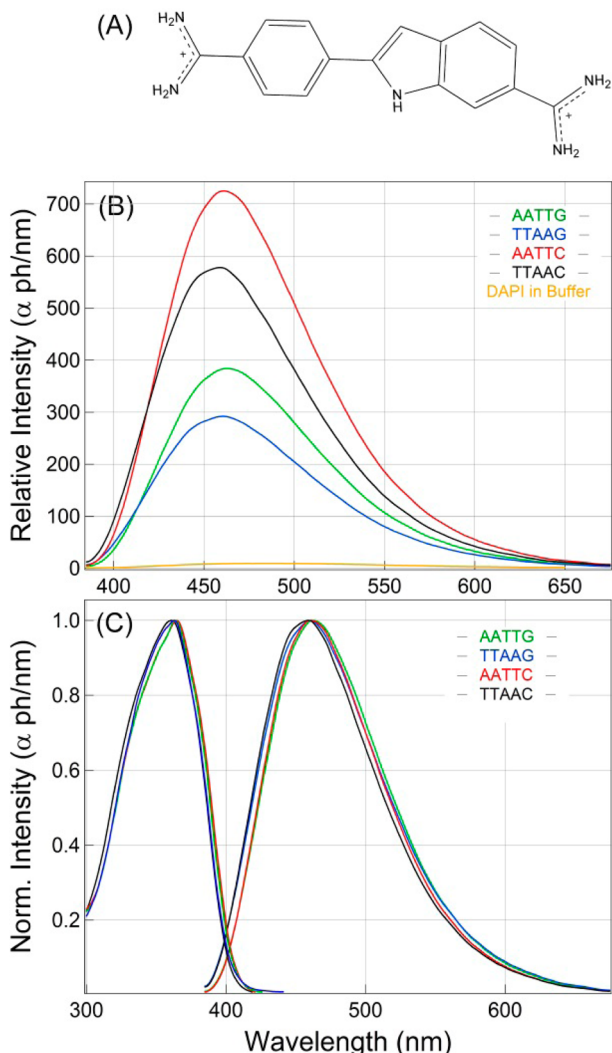


Figure 1. (A) Molecular structure of DAPI. (B) Fluorescence spectra (corrected) of DAPI in buffer and bound to minor-grooves of DNA formed by four different sequences. Spectra show sequence-dependent change in relative fluorescence intensities. See figure for legends. (C) Same emission spectra, normalized to one, showing the relative peak-shifts and shapes. The plot also includes excitation spectra of the same samples, which show similar trend as in emission spectra.

DAPI-fluorescence reaches saturation. Fluorescence spectra were collected using Varian Cary Eclipse fluorometer and corrected using quinine sulfate standard. Finally, the spectra are plotted as photon/nm vs nm or photons/cm⁻¹ vs cm⁻¹. UPC measurements (using FOG-100, CDP, pumped with Mai-TaiHP, Spectra-Physics) were carried out at concentrations [DAPI] = 20 μ M and [DNA] = 100 μ M (DAPI/DNA = 1:5). TCSPC measurements (using FL-920, Edinburgh Instruments) were conducted with samples of concentrations [DAPI] = 3 μ M and [DNA] = 15 μ M (DAPI/DNA = 1:5). The time-resolutions (IRF) of UPC and TCSPC setup were ~270 fs and ~100 ps, respectively. The time-zero glass spectra were measured by freezing the samples at -78 °C, similar as discussed earlier.^{5,48} Transparent glass was prepared by mixing glycerol in buffer at ratio 1:2 (buffer/glycerol). The solutions were then frozen in dry ice/acetone mixture at -78 °C and fluorescence spectra were measured. Finally, the “absolute” Stokes shifts were calculated by subtracting mean frequencies of

time-resolved emission spectra from the mean frequency of time-zero glass spectra.

RESULTS AND DISCUSSION

Steady-State Fluorescence Spectra. Steady-state fluorescence spectra provide direct information about the local solute–solvent interactions in solution. In water, the fluorescence quantum yield of DAPI is very low (~0.046),²⁷ which arises from nonradiative processes, possibly involving excited-state proton transfer at the indole ring of DAPI.⁶⁹ Upon binding to minor grooves of DNA, the DAPI fluorescence increases several fold. This increase occurs due to blocking of nonradiative proton transfer at the indole–NH as it involves in making bifurcated hydrogen-bond with DNA-bases.⁶ Figure 1 compares the (corrected) fluorescence and excitation spectra of DAPI bound to minor-grooves of DNA created by four different central base-sequences (see Figure 1A for DAPI structure). Upon binding to –AATTC–, DAPI shows the maximum fluorescence increment by ~75-fold compared to aqueous buffer (Figure 1B). The spectrum also shifts toward blue side (peak at ~461 nm) compared to buffer (peak at ~485 nm). Upon reversing the central sequence to –TTAAC– the intensity increases by ~58 times compared to buffer. The spectrum shows blue-shift by ~4 nm (peak at ~457 nm) compared to –AATTC– (see Figure 1B,C). Binding to –AATTG–, fluorescence increases by ~40 times, and in –TTAAG– the intensity increases by only ~30 times, relative to buffer. The fluorescence peak position (peak at ~460 nm) in –TTAAG– shows blue shift by ~3 nm compared to that in –AATTG– (peak at ~463 nm). Similar trend can be seen in the excitation spectra of DAPI in all sequences (Figure 1C). These observations indicate that DAPI senses a bit lower polarity inside DNA containing TTAA compared to AATT sequence (see Figure 1C).

Figure 1B shows that there is an overall decrease in fluorescence intensities when DAPI binds to sequences with flanking ‘G’ compared to with flanking ‘C’. This can arise due to shifting of DAPI binding-site toward the flanking ‘G’, as found in X-ray and simulation studies.^{20,21} In such cases, the groove widening near flanking ‘G’ and the steric hindrance introduced by –NH₂ group of guanine may have some effect on the DAPI binding, which leads to lower fluorescence yield of DAPI in sequences with flanking ‘G’.^{20,21} Note that the X-ray or simulated structures of DAPI bound to –TTAAC– and –TTAAG– are not available in literature. However, we expect that DAPI binds to these sequences at positions similar to –AATTC– and –AATTG–. In fact, the relative difference in fluorescence intensities does indicate such binding mode of DAPI to –TTAAC– and –TTAAG– compared to their AATT counterparts. Figure 1A also shows that there is a relative difference in fluorescence yields in grooves with central AATT and TTAA sequences, be it with flanking ‘C’ or ‘G’. A careful comparison of data also finds that the intensity difference is similar (~1.3-fold) among these sequences. This could possibly arise due to differences in groove-widths of DNA with central AATT and TTAA. Previous NMR studies showed that groove-width widens in duplex-DNA having TA-steps compared to AT-steps.^{63,64} The smaller groove-width near AATT can actually accommodate DAPI with stronger van der Waals interaction at the floor of minor-groove, which can lead to higher fluorescence yields of DAPI in DNA containing AATT compared to TTAA. In fact, previous stopped-flow experiments showed binding affinity of DAPI to AATT is much higher (~28

times) compared to TTAAC, which also supports our observations.¹⁹ Overall, the fluorescence spectra are implicative that DAPI interacts differently with different sequences, which facilitates the variation in static solvation structures around DAPI inside minor-grooves created by different base-sequences.

Figure 2 plots the steady-state fluorescence spectra (in frequency scale) at room temperature along with the time-zero

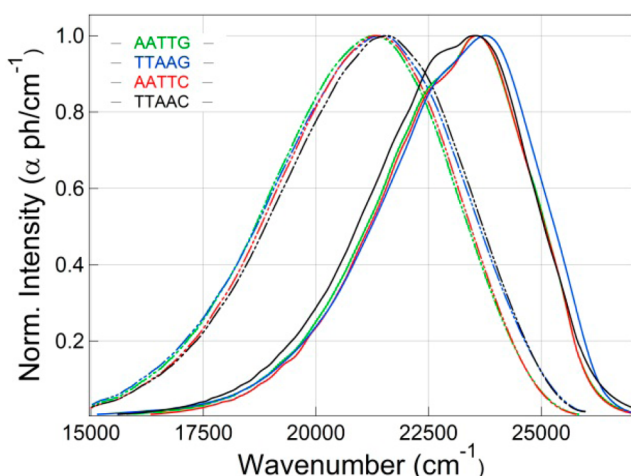


Figure 2. Time-zero glass spectra of DAPI in DNA of different sequences measured in dry ice/acetone mixture at $-78\text{ }^{\circ}\text{C}$ (solid lines). Fluorescence spectra of the DNA-samples at room temperature ($25\text{ }^{\circ}\text{C}$) are also plotted (dashed-dot) to show the amount of steady-state Stokes shifts relative to the time-zero position. At room temperature, the diffusive solvation dynamics continues beyond this time-zero position.

spectra of DAPI in DNA with different sequences in frozen-glass measured in dry ice/acetone mixture at $-78\text{ }^{\circ}\text{C}$.²⁸ The frozen-glass spectrum represents time-zero position of the solvation dynamics because in glass all diffusive dynamics of the sample are frozen, although vibrational and phonon-like inertial motions can persist.^{5,46–49} Thus, the glass spectrum provides an accurate measure of the time-zero position from where diffusive solvation dynamics starts in room temperature. It is evident from Figure 2 that both time-zero and room-temperature spectra of DAPI in minor-groove formed by --TTAAC-- stands out to be different compared to others. Moreover, the amount of static (time-averaged) Stokes shift at room-temperature, compared to glass spectrum, is less for the case of --TTAAC-- . Thus, one would expect to observe large deviation in the dynamic Stokes shift of DAPI bound to this sequence compared to others. In fact, we do observe such deviation in the dynamics for this sequence (see below).

Fluorescence Decays. In order to follow the sequence-dependent solvation dynamics in DNA over broad time range, we measured wavelength-dependent fluorescence decays of DAPI in minor-grooves created by different sequences using fluorescence up-conversion (UPC) and time-correlated single photon counting (TCSPC) techniques. In total, 20–22 fluorescence decays were measured in UPC and TCSPC for each sample. Decays show characteristic feature of solvation dynamics, that is, fast decay at blue-ends, fast-rise followed by slow decay near peak wavelengths, and slow-rise followed by slow decay at red-ends (see Figure S2 in Supporting Information for all decays). A sum of 4–5 exponentials is used to fit the decays, and the fitted parameters are used for further construction of time-resolved emission spectra (see below). Figure 3 compares the decays at blue-end, peak-region, and red-end, measured in TCSPC setup, which unfolds the sequence-dependent effects on raw fluorescence transients. It

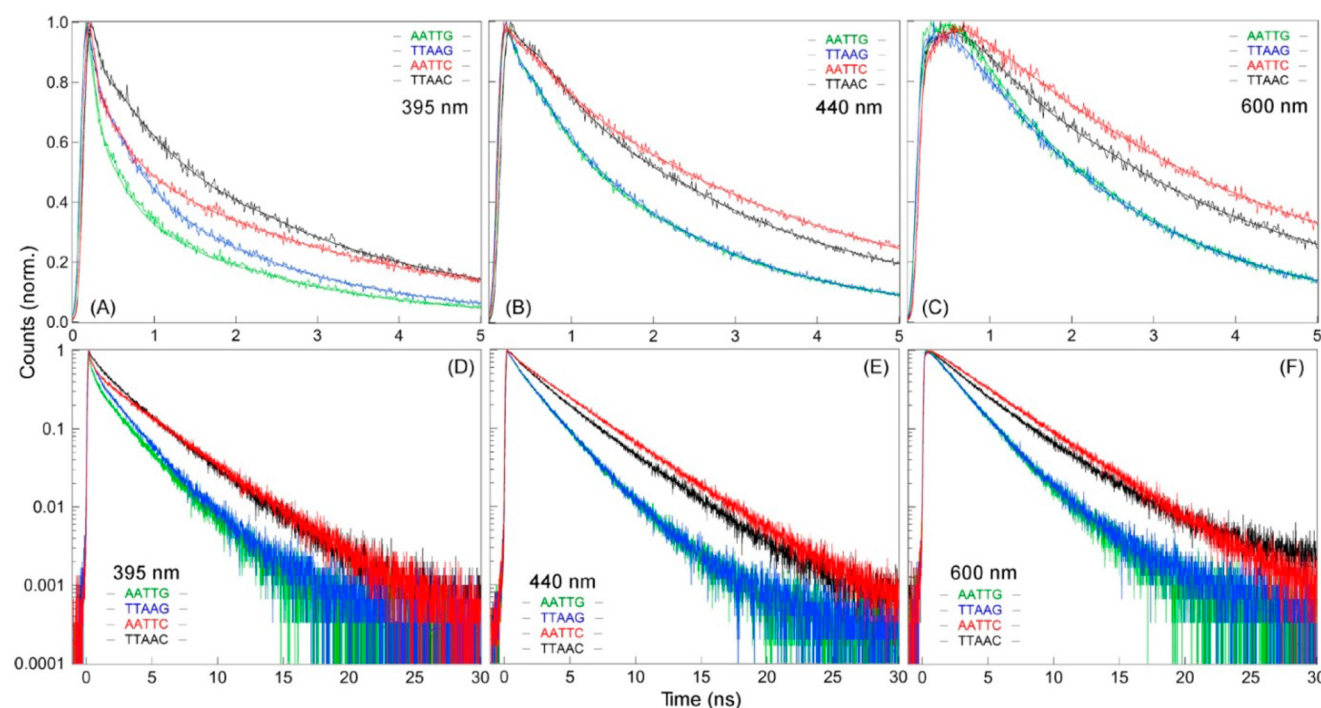


Figure 3. Fluorescence decays measured in TCSPC at blue-end, near peak region, and red-end of the fluorescence spectra of DAPI bound to DNA minor-grooves formed by --AATTG-- , --TTAAG-- , --AATTC-- , and --TTAAC-- . Top panels show data in short time-range up to 5 ns (A–C), and bottom panels show same data in full time-range in semilog plot (D–F). Figures also plot fits to the data.

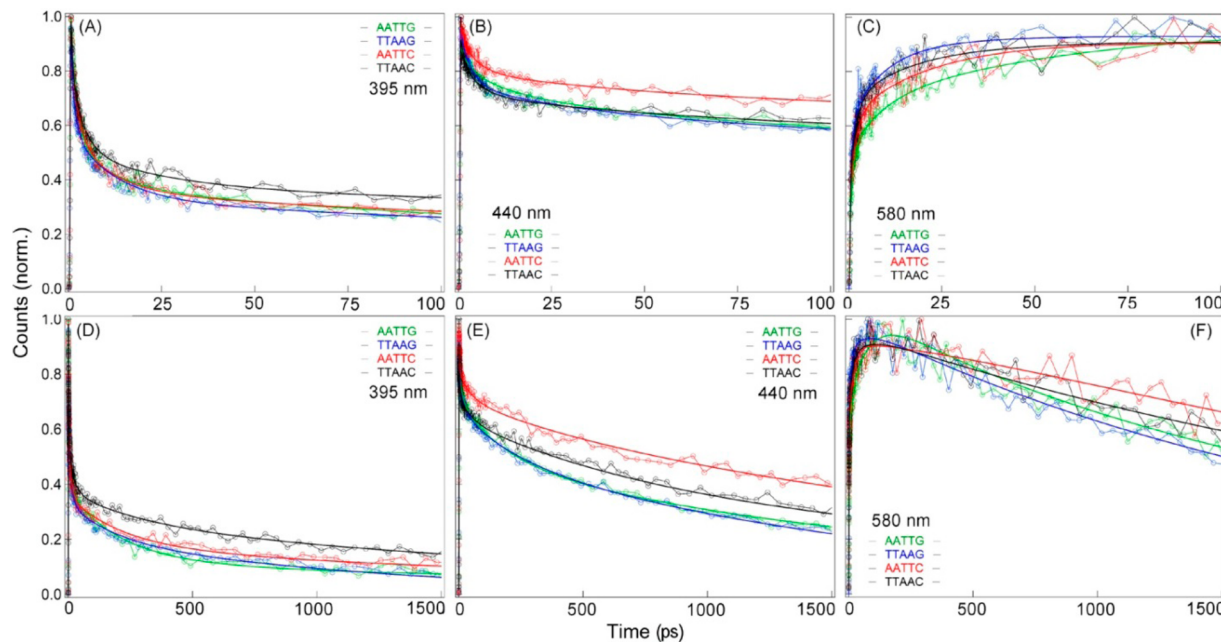


Figure 4. Fluorescence decays measured in UPC at blue-end, near peak region, and red-end of the fluorescence spectra of DAPI bound to DNA minor-groove formed by $-AATTG-$, $-TTAAG-$, $-AATTC-$, and $-TTAAC-$. Top panels show data in short time-range up to 100 ps (A–C), and bottom panels show same data in full measurable time-range up to 1.5 ns (D–F). Figures also plot fits to data.

can be seen that at peak and red wavelength regions the decays in DNA containing $-AATTG-$ and $-TTAAG-$ are similar. However, there is a subtle difference in decay rates in blue wavelength region. The central sequences with flanking ‘C’ induce the local dynamics of DAPI such that they show substantial sequence-dependence on fluorescence decays at all wavelengths. These raw decays clearly suggest that there is substantial difference in nanosecond solvation dynamics of DAPI in minor-grooves with different sequences, albeit similar in sequences with flanking ‘G’. Figure 4 compares the raw fluorescence transients in faster time-scales, measured in UPC setup. A similar sequence-dependent trend is seen in these decays as well. Nevertheless, the quantitative sequence-dependent effect on dynamics is captured in the dynamic Stokes shifts of DAPI, calculated from time-resolved emission spectra.

Time-Resolved Emission Spectra. The dynamics in DNA spreads over several decades in time from femtoseconds to nanoseconds.³⁴ To cover such broad time-range, we combine time-resolved emission spectra (TRES) of DAPI in DNA, constructed from fitted parameters of decays measured in fluorescence up-conversion (UPC; TRES range: 100 fs to 1 ns) and time-correlated single photon counting (TCSPC; TRES range: ~30 ps to 10 ns). The TRES data obtained from UPC and TCSPC techniques were merged in a self-consistent manner at common time-points of the two techniques in a similar way as discussed earlier.^{5,48} Figure 5 shows the TRES of DAPI in the minor-grooves of DNA formed by the four different base-sequences. Log-normal fits to TRES are used for calculating the time-dependent Stokes shifts in terms of first moment (mean) frequency shifts. The “absolute” Stokes shifts were then calculated by subtracting mean frequencies of TRES from the mean frequency of glass-spectra. (Note that the TRES of DAPI in minor-groove of DNA created by sequence $-AATTG-$ have been reported previously by us.^{5,48} However, a new set of data for the same DAPI-DNA system is also

obtained here for completeness. The results are found to be almost identical to that reported previously.^{5,48})

Comparison of Dynamic Stokes Shift Data. Dynamic Stokes shift studies with probes placed inside duplex-DNA either by covalent attachment or by minor groove-binding have been performed, which provided important information on DNA solvation dynamics from subpicosecond to nanoseconds time-scales.^{5,40,41} Berg and co-workers measured dynamic Stokes shifts of a covalently attached base-stacked coumarin (opposite an abasic-site) and showed that DNA dynamics extend into nanosecond time-scales.⁴¹ Zewail and co-workers reported TRFSS of a base-stacked probe (2-aminopurine) and a minor-groove bound ligand (Hoechst) to show that both probes sense similar dynamics inside DNA within 100 ps time-scale.^{42,43} Ernsting and co-workers also reported dynamics of base-stacked probe (HNF) until 25 ps and indicated that water controls the local dynamics inside duplex-DNA.⁴⁴ Pal and co-workers reported nanosecond solvation dynamics of groove-bound probes, DAPI and Hoechst, inside DNA minor-grooves,⁴⁵ showing that dynamics follow biexponential decay. However, combining Stokes shift data of base-stacked coumarin from different techniques, Berg and co-workers found that solvation dynamics in duplex-DNA actually follow a power-law relaxation with exponent 0.15 from 40 fs to 40 ns.^{46,47} Recently, we have reported the dynamic Stokes shift of DAPI inside the minor-groove of DNA formed by $-AATTG-$ and showed that the dynamics follow similar power-law as in case of base-stacked coumarin until ~100 ps,^{46,47} but beyond this time the dynamics converge rapidly to an equilibrium near 10 ns following biexponential decay.⁴⁸ Nonetheless, for sequence-dependent solvation dynamics in DNA, it is not known how the different AT-/TA-sequences affect the solvation of ligand inside DNA minor-grooves.

Figure 6A compares the “absolute” Stokes shifts of groove-bound DAPI in minor-grooves formed by the four different sequences. This plot reveals that (within error limit) the overall relative rates of Stokes shifts of DAPI are somewhat similar in

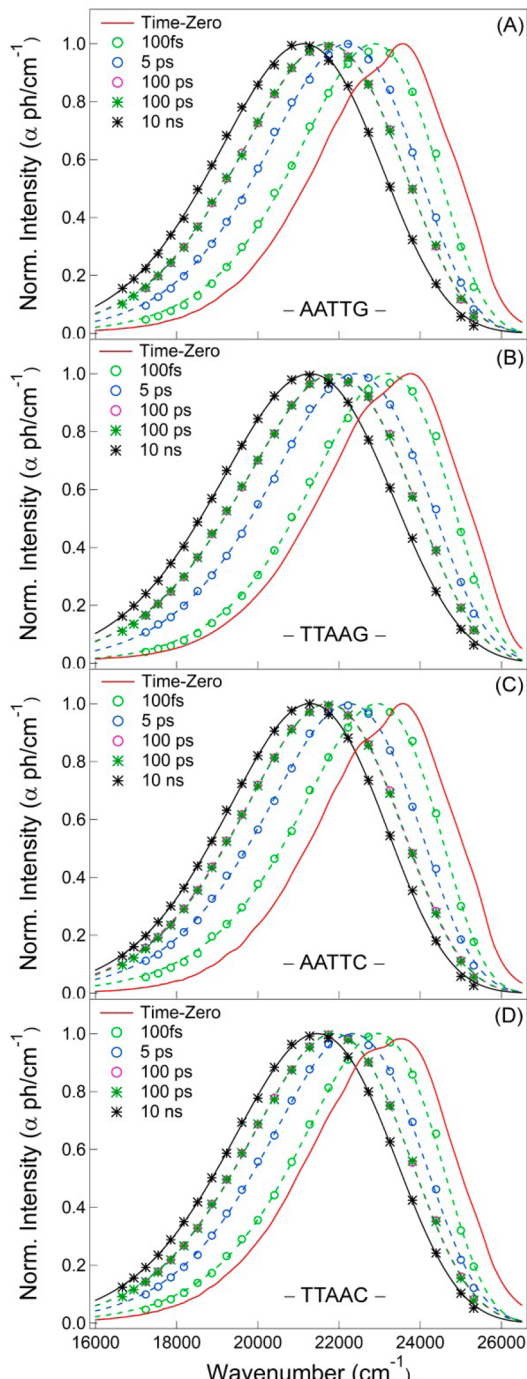


Figure 5. TRES of DAPI constructed from fluorescence decays measured in UPC (circles) and TCSPC (stars) in DNA with four different sequences. Matching of TRES from UPC and TCSPC at a common time-point (100 ps) is shown in figures. Dashed and solid lines denote log-normal fits. Red solid curves are time-zero glass spectra of the samples measured in dry ice/acetone mixture at -78°C (see text for details).

DNA having $-\text{AATTG}-$, $-\text{TTAAC}-$, and $-\text{AATTC}-$ sequences. However, the Stokes shift dynamics drastically changes when a single base (and the complementary base) is changed from $-\text{TTAAG}-$ to $-\text{TTAAC}-$. In fact, steady-state fluorescence spectra at room temperature and in frozen-glass do show some characteristic features in this sequence compared to others (see Figure 2). The comparison of Stokes shift data in

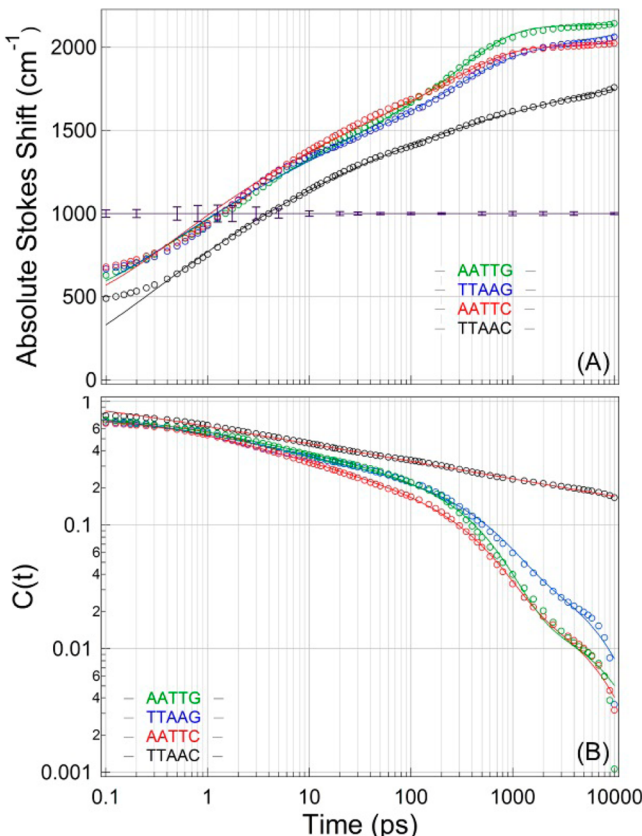


Figure 6. (A) Comparison of “absolute” Stokes shifts of DAPI from 100 fs to 10 ns in DNA minor-grooves formed by four different sequences. Plot includes error bars calculated from repeated measurement on a single DNA sequence. Error bars at few time-points covering the entire time-range have been included separately to minimize clumsiness (see Figure S3A in Supporting Information for error bars at all time-points). Error bars (SD) range from ± 5 to ± 50 cm^{-1} at different time-points. (B) Comparison of solvation correlation function, $C(t)$ of DAPI in minor-grooves of DNA, constructed from Stokes shift data in panel A as $C(t) = (S_{\infty} - S(t))/S_{\infty}$, plotted in log-log scale. Plots include fits to the data using either a single power-law or power-law multiplied with sum-of-two exponential functions (see text for details).

Figure 6A and the observed change in dynamics among different sequences is valid only if one has the knowledge of relative errors in the data. To validate our observation we calculated the error bars (standard deviations, SD) at each time point from several independently measured Stokes shift data of DAPI in a single sequence (i.e., $-\text{AATTG}-$), which are already reported^{5,48} (including the present data), and these data were taken over several years in different samples (see Supporting Information for details). This way one can exactly calculate the errors in Stokes shift data with time-delay. Figure 6A includes the error bars ($\pm \text{SD}$) at few time-points to minimize clumsiness (see Figure S3A in Supporting Information for error bars at all time-points). Clearly, the data confirms that the observed relative difference in Stokes shift dynamics of different sequences is real. The inherent Stokes shift dynamics of DAPI in $-\text{TTAAC}-$ suggests an unusual collective dynamics of water and DNA-proper (and possibly ions) around DAPI in minor-groove created by this sequence. Earlier stopped-flow kinetic study found that DAPI binds least strongly to the $-\text{TTAAC}-$ sequence compared to other combinations of this sequence.¹⁹ This could suggest that DAPI binding-site near this

sequence is rather different compared to others. In fact, our data suggests that change in single base near the ligand-binding site can actually induce the ligand environment near the groove in such a way that the ligand senses drastically different electrostatic interactions with nearby water, DNA-parts, and possibly ions. Although $-TTAAC-$ influences the DAPI solvation drastically, we also find subtle difference in dynamics in DNA with the other three sequences. This is realized clearly by analyzing the dynamic Stokes shift data.

Previously, we have reported the dynamic Stokes shift of groove-bound DAPI in DNA with central $-AATTG-$ sequence,⁴⁸ which we could model nicely with a power-law multiplied with the sum of two exponentials.⁴⁸ In fact, we find that the Stokes shift dynamics of DAPI in all three sequences, $-AATTG-$, $-TTAAG-$, and $-AATTC-$, can be nicely modeled with the same function (eq 1).⁴⁸

$$S(t) = S_{\infty} \left[1 - \left(1 + \frac{t}{t_0} \right)^{-n} (a_1 e^{-t/\tau_1} + a_2 e^{-t/\tau_2}) \right] \quad (1)$$

In eq 1, $S(t)$ is the time-dependent absolute Stokes shift, S_{∞} is the parameter that extract Stokes shift at infinite time, t_0 is the time below which power-law converges to zero, n is power-law exponent, and a_1 and a_2 are contributions of two exponential time-constants, τ_1 and τ_2 , respectively. The fitted parameters for $-AATTG-$, $-TTAAG-$, and $-AATTC-$ are listed in Table 1.

Table 1. Parameters Obtained from Fitting of Absolute Stokes Shift Data Using Eqs 1 and 2

sequence	S_{∞} (cm ⁻¹)	n	t_0 (ps)	a_1	τ_1 (ps)	a_2	τ_2 (ns)
$-AATTG-$	2140	0.15	0.09	0.76	460	0.05	6.0
$-TTAAG-$	2092	0.16	0.08	0.49	455	0.32	6.0
$-AATTC-$	2028	0.20	0.08	0.70	450	0.13	6.0
$-TTAAC-$	2107	0.14	0.05				

However, the dynamics in $-TTAAC-$ is singled out, which is found to follow a single power-law type relaxation over the entire time range and the dynamics continues beyond the longest time measured (10 ns). Hence, $-TTAAC-$ data is fitted with a power-law⁴⁷

$$S(t) = S_{\infty} \left[1 - \left(1 + \frac{t}{t_0} \right)^{-n} \right] \quad (2)$$

The fitted parameters for $-TTAAC-$ are also listed in Table 1. Note that the fitting below ~ 200 fs is less satisfactory. This arises due to limited time-resolution of our UPC setup (~ 270 fs), which could not extract the full dynamics in faster time-scales (see Figure 6A). In fact, due to limited time-resolution we missed ~ 500 – 700 cm⁻¹ of Stokes shifts at 100 fs in all data. Fitted parameters show subtle difference in solvation of DAPI in the cases of $-AATTG-$, $-TTAAG-$, and $-AATTC-$, while a drastic difference is observed in the case of $-TTAAC-$ (see Table 1). One should note at this point that in solvation dynamics studies the general practice has been to consider S_{∞} the same as the dynamic Stokes shift at the longest measurable time or the frequency of the dynamic spectrum that matches steady-state fluorescence spectrum. This can be done only if the dynamics of the system completes within the measured time-window of experiment, which is generally limited by the fluorescence decay-time of the probe used. However, previous

experiments found that dynamics in DNA extends over several time-decades, which continue beyond the maximum measurable time of fluorescence Stokes shift of a given probe.^{34,46–49} Simulation studies also support this finding.^{70,74} The same is true in the present case, at least for $-TTAAC-$ where the dynamics is found to continue smoothly until 10 ns and beyond, while the dynamics in the other three sequences shows plateau beyond ~ 2 ns. Thus, the use of S_{∞} as a free parameter in eqs 1 and 2 is justified because it provides an estimate for total Stokes shift when the system reaches equilibrium. This extrapolation in longer times is justified because we already captured 85% of (power-law) dynamics until 10 ns in $-TTAAC-$, while more than 99% of dynamics is captured in the case of the other three sequences. Nevertheless, we tested this hypothesis by fixing S_{∞} values the same as the Stokes shifts at the longest time (10 ns) in the fitting analysis using eqs 1 and 2. The fits to data of $-AATTG-$, $-TTAAG-$, and $-AATTC-$ do not change much, as we already captured more than 99% of the dynamics in these three sequences. However, the fit to $-TTAAC-$ data is not satisfactory (see Figure S3B in Supporting Information). This is because the dynamics in $-TTAAC-$ continues beyond 10 ns, and fixing S_{∞} value as the Stokes shift at 10 ns suddenly truncate the dynamics. Hence, the fitted S_{∞} values obtained in Table 1 are reliable.

To show the power-law and multiexponential relaxations clearly, Figure 6B constructs the solvation correlation function, $C(t)$, from the absolute Stokes shift data as $C(t) = (S_{\infty} - S(t))/S_{\infty}$, in log–log plot. This plot clearly shows that the dynamics in $-TTAAC-$ follows a single power-law (with exponent 0.14) over the entire time range. However, in the other three sequences the solvation dynamics follows a power-law in the initial decades, but beyond ~ 100 ps the dynamics switch to multiexponential relaxation, which rapidly reaches equilibrium near 10 ns (see also Table 1).

In order to better understand the sequence-dependent solvation dynamics in DNA, comparisons of $C(t)$ of DAPI and previously reported base-stacked coumarin^{46,47} are made separately in Figure 7. Figure 7A compares the $C(t)$ of DAPI bound to central sequences with flanking ‘G’ (i.e., $-AATTG-$ and $-TTAAG-$) and the base-stacked coumarin data.^{46,47} In fact, this plot compares the sequences where DAPI binds preferentially toward flanking ‘G’; near ATTG and TAAG. Earlier X-ray and MD simulation studies found such binding site of DAPI.^{20,21} Figure 7A unfolds that Stokes shift dynamics in these two sequences follow power-law relaxation (of exponent 0.15 and 0.16) in initial three decades, very similar as observed earlier for base-stacked coumarin (exponent 0.15).^{46,47} However, the power-law dynamics of DAPI in both sequences deviate beyond ~ 100 ps and switch to multiexponential relaxation to converge rapidly toward equilibrium. The sequence dependence on the dynamics can only be seen in the last time-decade (~ 1 – 10 ns), where the contribution of the longest component (6 ns) becomes larger in the case of $-TTAAG-$ compared to $-AATTG-$, and subsequent decrease in contribution of fast component (see Table 1).

The most unusual sequence dependence on solvation dynamics of DAPI is captured in Figure 7B, which compares the $C(t)$ of DAPI in $-AATTC-$ and $-TTAAC-$ and that of base-stacked coumarin.^{46,47} It can be seen that dynamics in $-AATTC-$ follows power-law relaxation of exponent 0.2 in initial time-decades, followed by multiexponential relaxation in longer times (see Table 1). When compared to the dynamics of

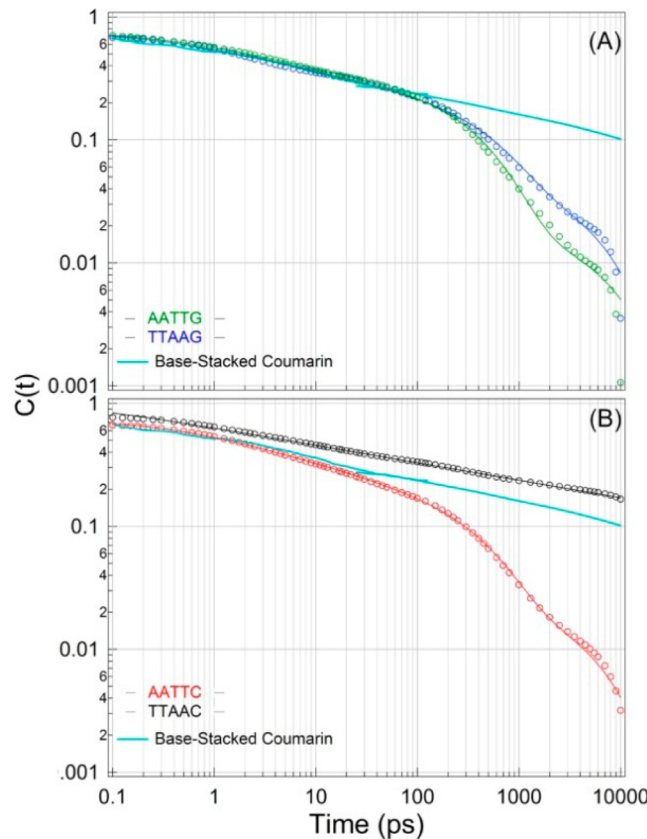


Figure 7. Comparison of solvation correlation function, $C(t)$, of DAPI in DNA containing (A) -AATTG- and -TTAAG-, (B) -AATTC- and -TTAAC-, constructed from Stokes shifts data in Figure 6A (open circles), plotted in log-log scale. For comparison, plots also include the previous base-stacked coumarin data reported by Berg and co-workers (cyan solid line).^{46,47} Fits to DAPI data are included. The $C(t)$ of DAPI in -TTAAC- is almost parallel to the coumarin data, which follow a single power-law over the entire time-range.

base-stacked coumarin,^{46,47} the dynamics of DAPI in -AATTC- is found to deviate from coumarin data at ~ 10 ps, instead of ~ 100 ps as seen in the case of -AATTG- or -TTAAG- because of larger exponent (0.2) of power-law relaxation in initial time-decades. Nonetheless, the most severe sequence effect on the dynamics is found in -TTAAC-, which shows a single power-law relaxation (with exponent 0.14) over the entire time-range. The dynamics is found to be almost parallel to the coumarin data (Figure 7B).^{46,47} This finding is unusual in a sense that it is quite unexpected to have such an enormous effect on solvation dynamics by only reversing the central AATT sequence to TTAA with flanking "C", but not with flanking "G". More importantly, comparing -TTAAG- and -TTAAC- data, it is found that the most severe sequence effect occurs when the flanking base is changed from 'G' to 'C' in central TTAA sequence. Interestingly, however, the amazing similarity in dynamics of minor-groove bound DAPI in -TTAAC- and base-stacked coumarin (opposite an abasic-site) in a generic sequence clearly proves the generality of highly dispersed power-law solvation dynamics in DNA.

The data presented here raise several questions: What is the origin of dispersed power-law solvation of DNA-bound ligand inside minor grooves? Is it the motion of water, or DNA, or ions, or is it their coupled motion that controls the anomalous sequence-dependent dynamics in minor-grooves of DNA? The

answers are not known yet. However, reconciling current understanding of DNA-solvation from experiments and simulations as well as the available structural information on DNA, we put forward some reasonable explanations for origin of dispersed sequence-dependent dynamics in DNA, which may be tested further by simulations and experiments.

Previously (and also here) we compared the DNA-dynamics probed by groove-bound DAPI in -AATTG- and base-stacked coumarin in generic-sequence reported by one of us with Berg and co-workers.⁴⁸ Reconciling earlier MD simulation results on DNA solvation dynamics reported by Sen et al.,⁷⁰ Bagchi-Hynes and co-workers,⁷¹ and Furse and Corcelli,^{72–74} we propose that, because DAPI binding to the minor-groove of DNA is entropically favored by displacing water and ions from the grooves, the groove-bound DAPI may not sense the slow water and ion motions. However, the base-stacked coumarin can sense the slow hydration and ion dynamics in-and-around DNA, which may lead to the observed power-law dynamics.^{46,47} In fact, analyzing long MD trajectories of native-DNA and comparing the experimental data of coumarin with simulation, Sen et al. found that the slow water controls the dispersed power-law dynamics in DNA, albeit with small but appreciable contribution from ion-motions.⁷⁰ However, when Furse and Corcelli simulated the duplex-DNA with coumarin and abasic pair, similar to that used in experiment of Berg and co-workers, they saw substantial contribution from the abasic-site flipping motion to the longtime power-law dynamics.⁷⁴ Hence, they proposed that it is the DNA abasic flipping motion, rather than the water motion, which controls the power-law solvation dynamics in DNA.⁷⁴ Along this line, one possibility could be that the observed power-law dynamics of DAPI in -TTAAC- in times longer than 100 ps may arise from the local motions of DNA-bases or from the coupled motions of bases and local hydration-water (see below). Using mode-coupling theory, Bagchi has also suggested that the collective ion-motions around DNA can contribute to dictate the power-law solvation dynamics in DNA.⁷⁵ However, the DAPI binding to minor grooves of DNA displaces most of the slow water and ions from the grooves. In fact, Furse-Corcelli simulated groove-bound Hoechst and found that it is the DNA motion that controls the slow dynamics sensed by the ligand, while water only contributes to the fast relaxation and ions have negligible or no effect on the dynamics.⁷² This observation is in line with the groove-bound DAPI data presented here. Furthermore, through comparison of ion-dependent TRFSS results of DAPI inside minor-groove formed by -AATTG- we also showed earlier that DAPI can not sense the ion motions when it is bound inside minor-groove.⁵ Hence, one would not expect to observe large ion contribution to the total dynamics sensed by DAPI when bound to minor-grooves created by different sequences. In fact, the dicationic DAPI should actually screen the positively charged ions from coming close to DAPI-binding site. Nonetheless, it is still difficult to explain the seemingly similar power-law dynamics sensed by groove-bound DAPI in -TTAAC- and base-stacked coumarin in generic sequence as well as the different dynamics sensed by DAPI in the other three sequences.

The structural and MD simulation studies on DNA provide some clues to further explain the observed sequence-dependent solvation dynamics in DNA. In an early NMR study, Otting and co-workers found that reversing the central AATT sequence to TTAA actually induces the minor groove-width and the hydration structure inside the grooves.⁶³ They found

structured water with long residence times in the smaller groove of AATT, whereas the wider TTAA-groove does not contain such structured water.⁶³ However, this finding was challenged by Johannesson and Halle showing in a NMR study that despite having wider groove TA-step can also have structured water with long residence times.⁷⁶ Through rigorous structural analysis of nucleic acid database Dickerson and co-workers also pointed out that AT-steps display negative role with a slight bend toward the minor groove, while TA-steps show positive role, which bent toward the major groove. This leads to the widening of minor grooves created by TA-steps.⁶⁴ Furthermore, NMR data suggested that slow conformational dynamics is a feature common to all TA-steps inside DNA.⁷⁷ In a recent QENS and simulation study, Nahagawa et al. also found that the dynamics in DNA containing –AATTC– and –TTAAC– are related to the local base-pair dynamics, which is coupled to the hydration water inside the minor grooves.⁶⁶ Relating the observed variations in groove-widths, local DNA-motions, and DAPI binding sites in different sequences, we therefore infer that the perturbation due to ligand-binding to minor-grooves of different sequences should have severe effect on the local hydration structure near the ligand. Along this line, it is expected that DAPI binding to a groove of –AATTG– or –TTAAG– should experience different local hydration dynamics, which is coupled to the local DNA-motions. However, the small variations in slow dynamics in these two sequences also indicate that the relative groove-widths near the DAPI binding-site are not drastically different as the binding site shifts by one base toward the major groove in these sequences. Nonetheless, because of larger groove-width of DNA containing TTAA sequence, the ligand may stay exposed more toward the outside environment, which may induce larger interaction of the ligand with nearby perturbed (slow) water. Such situation can affect the slow multiexponential relaxation in long times as seen here (see Table 1). However, the unusual dynamic behavior in –TTAAC– may originate from substantial change in the groove-width near the DAPI binding-site by going from –AATTC– to –TTAAC–. Because DAPI preferentially binds to the central AATT or TTAA region in these sequences, and not toward wider major-groove as in other two sequences, DAPI can experience a severe widening of groove-width on going from AATT to TTAA with the flanking ‘C’. This may lead to substantial change in the contribution from surrounding water and DNA-parts within few angstroms of the ligand, possibly with larger contribution from the water. Another possibility could be that the inherent conformational flexibility of TA-steps, coupled with the local hydration dynamics,⁶⁶ dictate the highly dispersed power-law solvation of DAPI in the minor-groove of –TTAAC–.

CONCLUSION

The fact that ligand binding to DNA-grooves depends on the base-sequence is already well-established. However, it was not known how far such sequence-dependent binding of ligands influence the local solvation structure and dynamics around the ligands inside grooves of DNA. This article sheds light on such complex behavior of ligand solvation inside DNA minor-grooves created by different base-sequences. The ligand solvation dynamics is shown to vary drastically depending on the base-sequence, which relates to the different binding modes of ligand in different sequences and (possibly) the sequence-dependent variation of local DNA motions, coupled with local hydration dynamics. The change in ligand solvation is found to

depend on single-base (and complementary base) variation near the ligand binding-site. The results presented here also have important implications in the sequence-dependent protein binding to DNA. In fact, similar sequence-dependent solvation is expected to persist near the protein-binding sites inside DNA. Such change in local-solvation and its dynamics (at single base-level) perhaps helps proteins to recognize sequence-dependent DNA-binding sites. Nevertheless, the most fascinating fact to note here that time-resolved fluorescence Stokes shift experiments have remarkable ability to discern the minute differences in dynamics even at (single) base level, although the exact origin of the observed sequence-dependent dynamics is still unclear. Certainly, further MD simulation and experimental studies are necessary to find the exact origin of the observed sequence-dependent solvation dynamics in DNA. In fact, some such studies are underway in our laboratory, and we hope to shed more light on this problem in our future communications.

ASSOCIATED CONTENT

Supporting Information

Circular dichroism (CD) spectra; wavelength-dependent fluorescence decays; calculation of errors in Stokes shift data. The Supporting Information is available free of charge on the ACS Publications website at DOI: 10.1021/acs.jpcb.5b01977.

AUTHOR INFORMATION

Corresponding Author

*E-mail: sens@mail.jnu.ac.in.

Notes

The authors declare no competing financial interest.

ACKNOWLEDGMENTS

This work is supported by Department of Science and Technology (SR/FTP/PS-16/2007 and DST-FIST) and Department of Biotechnology (DBT-BUILDER). We thank Dr. P. Mukhopadhyay (SPS, JNU) for the use of fluorometer. UPC, TCSPC, and CD data were collected at AIRF, JNU. S.D.V. thanks UGC, and N.P. and M.K.S. thank CSIR for fellowships.

REFERENCES

- (1) Tidwell, R. R.; Boykin, D. W. *DNA and RNA Binders: From Small Molecules to Drugs*; WILEY-VCH: Germany, 2003.
- (2) Midgley, I.; Fitzpatrick, K.; Taylor, L. M.; Houchen, T. L.; Henderson, S. J.; Cybulski, Z. R.; John, B. A.; McBurney, A.; Boykin, D. W.; Trendler, K. L. Pharmacokinetics and metabolism of the prodrug DB289 (2,5-bis[4-(N-methoxyamidino)phenyl]furan dihydrochloride) in rats and monkey and its conversion to the antiprotozoal/antifungal drug DB75 (2,5-bis(4-guanylphenyl)furan hydrochloride). *Drug. Metab. Dispos.* **2007**, *35*, 955–967.
- (3) Wilson, W. D.; Nguyen, B.; Tanious, F. A.; Mathis, A.; Hall, J. E.; Stephens, C. E.; Boykin, D. W. Dications that target the DNA minor groove: compound design and preparation, DNA interactions, cellular distribution and biological activity. *Curr. Med. Chem. Anticancer Agents* **2005**, *5*, 389–408.
- (4) Nguyen, B.; Neidle, S.; Wilson, W. D. A role for water molecules in DNA-ligand minor groove recognition. *Acc. Chem. Res.* **2009**, *42*, 11–21.
- (5) Verma, S. D.; Pal, N.; Singh, M. K.; Sen, S. Probe position-dependent counterion dynamics in DNA: comparison of time-resolved stokes shift of groove-bound to base-stacked probes in the presence of different monovalent counterions. *J. Phys. Chem. Lett.* **2012**, *3*, 2621–2626.

- (6) Larsen, T. A.; Goodsell, D. S.; Cascio, D.; Grzeskowiak, K.; Dickerson, R. E. The structure of DAPI bound to DNA. *J. Biomol. Struct. Dyn.* **1989**, *7*, 477–791.
- (7) Han, F.; Taulier, N.; Chalikian, T. V. Association of the minor groove binding drug Hoechst 33258 with d(CGCAATTGCG)2: volumetric, calorimetric, and spectroscopic characterizations. *Biochemistry* **2005**, *44*, 9785–9794.
- (8) Haq, I.; Ladbury, J. E.; Chowdhury, B. Z.; Jenkins, T. C.; Chaires, J. B. Specific binding of Hoechst 33258 to the d-(CGCAAATTGCG)2 duplex: calorimetric and spectroscopic studies. *J. Mol. Biol.* **1997**, *271*, 244–257.
- (9) Furse, K. E.; Corcelli, S. A. The dynamics of water at DNA interfaces: computational studies of Hoechst 33258 bound to DNA. *J. Am. Chem. Soc.* **2008**, *130*, 13103–13109.
- (10) Spolar, R. S.; Record, M. T. Coupling of local folding to site-specific binding of proteins to DNA. *Science* **1994**, *263*, 777–784.
- (11) Williams, L. D.; Maher, L. J., 3rd Electrostatic mechanisms of DNA deformation. *Annu. Rev. Biophys. Biomol. Struct.* **2000**, *29*, 497–521.
- (12) Mukherjee, A.; Lavery, R.; Bagchi, B.; Hynes, J. T. On the molecular mechanism of drug intercalation into DNA: a simulation study of the intercalation pathway, free energy, and DNA structural changes. *J. Am. Chem. Soc.* **2008**, *130*, 9747–9755.
- (13) Bewly, C. A.; Gronenborn, A. M.; Clore, G. M. Minor groove-binding architectural proteins: structure, function, and DNA recognition. *Annu. Rev. Biophys. Biomol. Struct.* **1998**, *27*, 105–131.
- (14) Nekludova, L.; Pabo, C. O. Distinctive DNA conformation with enlarged major groove is found in Zn-finger-DNA and other protein-DNA complexes. *Proc. Natl. Acad. Sci. U.S.A.* **1994**, *91*, 6948–6952.
- (15) Jones, S.; van Heyningen, P.; Berman, H. M.; Thornton, J. N. Protein-DNA interactions: A structural analysis. *J. Mol. Biol.* **1999**, *287*, 877–896.
- (16) Oguey, C.; Foloppe, N.; Hartmann, B. Understanding the sequence-dependence of DNA groove dimensions: implications for DNA interactions. *PLoS One* **2010**, *5*, e15931.
- (17) Nag, N.; Rao, B. J.; Krishnamoorthy, G. Altered dynamics of DNA bases adjacent to a mismatch: a cue for mismatch recognition by mutS. *J. Mol. Biol.* **2007**, *374*, 39–53.
- (18) Rohs, R.; West, S. M.; Sosinsky, A.; Liu, P.; Mann, R. S. The role of DNA shape in protein-DNA recognition. *Nature* **2009**, *461*, 1248–1253.
- (19) Breusegem, S. Y.; Clegg, R. M.; Loontjens, F. G. Base-sequence specificity of Hoechst 33258 and DAPI binding to five (A/T)4 DNA sites with kinetic evidence for more than one high-affinity Hoechst 33258-AATT complex. *J. Mol. Biol.* **2002**, *315*, 1049–1061.
- (20) Vlieghe, D.; Sponer, J.; Meervelt, L. V. Crystal structure of d(GGCCAATTGG) complexed with DAPI reveals novel binding mode. *Biochemistry* **1999**, *38*, 16443–16451.
- (21) Spackova, N.; Cheatham, T. E., III; Ryjacek, F.; Lankas, F.; Meervelt, L. V.; Hobza, P.; Sponer, J. Molecular dynamics simulations and thermodynamics analysis of DNA-drug complexes. Minor groove binding between 4'-6-diamino-2-phenylindole and DNA duplexes in solution. *J. Am. Chem. Soc.* **2003**, *125*, 1759–1769.
- (22) Albert, F. G.; Eckdahl, T. T.; Fitzgerald, D. J.; Anderson, J. N. Heterogeneity in the actions of drugs that bind in the DNA minor groove. *Biochemistry* **1999**, *38*, 10135–10146.
- (23) Tawar, U.; Jain, A. K.; Chandra, R.; Singh, Y.; Dwarakanath, B. S.; Chaudhury, N. K.; Good, L.; Tandon, V. Minor groove binding DNA ligands with expanded A/T sequence length recognition, selective binding to bent DNA regions and enhanced fluorescent properties. *Biochemistry* **2003**, *42*, 13339–13346.
- (24) Trotta, E.; Grosso, N. D.; Erba, M.; Melino, S.; Cicero, D.; Paci, M. Interaction of DAPI with individual strands of trinucleotide repeats. Effects of replication in vitro of the AAT x ATT triplet. *Eur. J. Biochem.* **2003**, *270*, 4755–4761.
- (25) Niedle, S. DNA minor-groove recognition by small molecules. *Nat. Prod. Rep.* **2001**, *18*, 291–309.
- (26) Vega, M. C.; Saez, I. G.; Aymami, J.; Eritja, R.; Vandermarel, G. A.; Vanboom, J. H.; Rich, A.; Coll, M. 3-Dimensional crystal-structure of the a-tract DNA dodecamer d(CGCAAATTGCG) complexed with the minor-groove-Binding Drug Hoechst-33258. *Eur. J. Biochem.* **1994**, *222*, 721–726.
- (27) Spink, N.; Brown, D. G.; Skelly, J. V.; Neidle, S. Sequence dependent effects in drug-DNA interaction: the crystal structure of Hoechst 33258 bound to the d(CGCAAATTGCG)2 duplex. *Nucleic Acids Res.* **1994**, *22*, 1607–1612.
- (28) Abu-Daya, A.; Brown, P. M.; Fox, K. R. DNA sequence preferences of several AT-selective minor groove binding ligands. *Nucleic Acids Res.* **1995**, *23*, 3385–3392.
- (29) Wilson, W. D.; Tanius, F. A.; Barton, H. J.; Jones, R. L.; Fox, K.; Wydra, R. L.; Sterkowski, L. DNA sequence dependent binding modes of 4',6-diamino-2-phenylindole (DAPI). *Biochemistry* **1990**, *29*, 8452–8461.
- (30) Goodsell, D.; Dickerson, R. E. Isohelical analysis of DNA groove-binding drugs. *J. Med. Chem.* **1986**, *29*, 688–693.
- (31) Nguyen, B.; Hamelberg, D.; Baily, C.; Colson, P.; Stanek, J.; Brun, R.; Neidle, S.; Wilson, W. D. Characterization of a novel DNA minor-groove complex. *Biophys. J.* **2004**, *86*, 1028–1041.
- (32) Laughton, C.; Luisi, B. The mechanics of minor groove width variation in DNA, and its implications for the accommodation of ligands. *J. Mol. Biol.* **1998**, *288*, 953–963.
- (33) Pal, S. K.; Zewail, A. H. Dynamics of water in biological recognition. *Chem. Rev.* **2004**, *104*, 2099–2124.
- (34) Berg, M. A.; Coleman, R. S.; Murphy, C. Nanoscale structure and dynamics of DNA. *Phys. Chem. Chem. Phys.* **2008**, *10*, 1229–1242.
- (35) Bhattacharyya, K. Nature of biological water: a femtosecond study. *Chem. Commun.* **2008**, *25*, 2848–2857.
- (36) Jimenez, R.; Fleming, G. R.; Kumar, P. V.; Maroncelli, M. Femtosecond solvation dynamics of water. *Nature* **1994**, *369*, 471–473.
- (37) Samanta, A. Solvation dynamics in ionic liquids: what we have learned from the dynamic fluorescence stokes shift studies. *J. Phys. Chem. Lett.* **2010**, *1*, 1557–1562.
- (38) Liang, M.; Zhang, X.-X.; Kaintz, A.; Ernsting, N. P.; Maroncelli, M. Solvation dynamics in a prototypical ionic liquid + dipolar aprotic liquid mixture: 1-butyl-3-methylimidazolium tetrafluoroborate + acetonitrile. *J. Phys. Chem. B* **2014**, *118*, 1340–1352.
- (39) Li, T.; Hassanali, A. A.; Kao, Y.-T.; Zhong, D.; Singer, S. J. Hydration dynamic and time scales of coupled water-protein fluctuations. *J. Am. Chem. Soc.* **2007**, *129*, 3376–3382.
- (40) Chang, C.-W.; He, T.-F.; Guo, L.; Stevens, J. A.; Li, T.; Wang, L.; Zhong, D. Mapping solvation dynamics at the function site of flavodoxin in three redox states. *J. Am. Chem. Soc.* **2010**, *132*, 12741–12747.
- (41) Brauns, E. B.; Madaras, M. L.; Coleman, R. S.; Murphy, C. J.; Berg, M. A. Measurement of local DNA reorganization on the picosecond and nanosecond time scales. *J. Am. Chem. Soc.* **1999**, *121*, 11644–11649.
- (42) Pal, S. K.; Zhao, L.; Zewail, A. H. Water at DNA surfaces: Ultrafast dynamics in minor groove recognition. *Proc. Natl. Acad. Sci. U.S.A.* **2003**, *100*, 8113–8118.
- (43) Pal, S. K.; Zhao, L.; Xia, T.; Zewail, A. H. Site- and sequence-selective ultrafast hydration of DNA. *Proc. Natl. Acad. Sci. U.S.A.* **2003**, *100*, 13746–13751.
- (44) Dallmann, A.; Pfaffe, M.; Mügge, C.; Mahrwald, R.; Kovalenko, S. A.; Ernsting, N. P. Local THz time-domain spectroscopy of duplex DNA via fluorescence of an embedded probe. *J. Phys. Chem. B* **2009**, *113*, 15619–15628.
- (45) Banerjee, D.; Pal, S. K. Dynamics in the DNA recognition by DAPI: exploration of the various binding modes. *J. Phys. Chem. B* **2008**, *112*, 1016–1021.
- (46) Andreatta, D.; Sen, S.; Pérez Lustres, J. L.; Kovalenko, S. A.; Ernsting, N. P.; Murphy, C. J.; Coleman, R. S.; Berg, M. A. Ultrafast dynamics in DNA: "fraying" at the end of the helix. *J. Am. Chem. Soc.* **2006**, *128*, 6885–6892.
- (47) Andreatta, D.; Pérez Lustres, J. L.; Kovalenko, S. A.; Ernsting, N. P.; Murphy, C. J.; Coleman, R. S.; Berg, M. A. Power-law solvation

- dynamics in DNA over six decades in time. *J. Am. Chem. Soc.* **2005**, *127*, 7270–7271.
- (48) Pal, N.; Verma, S. D.; Sen, S. Probe position dependence of DNA dynamics: comparison of the time-resolved Stokes shift of groove-bound to base-stacked probes. *J. Am. Chem. Soc.* **2010**, *132*, 9277–9279.
- (49) Sen, S.; Gearheart, L. A.; Rivers, E.; Liu, H.; Coleman, R. S.; Murphy, C. J.; Berg, M. A. Role of monovalent counterions in the ultrafast solvation dynamics of DNA. *J. Phys. Chem. B* **2006**, *110*, 13248–13255.
- (50) Sajadi, M.; Furse, K. E.; Zhang, X.-X.; Dehmel, L.; Kovalenko, S. A.; Corcelli, S. A.; Ernsting, N. P. Detection of DNA–ligand binding oscillations by stokes-shift measurements. *Angew. Chem., Int. Ed.* **2011**, *50*, 9501–9505.
- (51) Yang, Y.; Qin, Y.; Ding, Q.; Bakhtina, M.; Wang, L.; Tsai, M.-D.; Zhong, D. Ultrafast water dynamics at the interface of the polymerase–DNA binding complex. *Biochemistry* **2014**, *53*, 5405–5413.
- (52) Sen, S.; Paraggio, N. A.; Gearheart, L. A.; Connor, E. E.; Issa, A.; Coleman, R. S.; Wilson, D. M., III; Wyatt, M. D.; Berg, M. A. Effect of protein binding on ultrafast DNA dynamics: Characterization of a DNA:APE1 complex. *Biophys. J.* **2005**, *89*, 4129–4138.
- (53) Zhong, D.; Pal, S. K.; Zewail, A. H. Femtosecond studies of protein-DNA binding and dynamics: histone I. *ChemPhysChem* **2001**, *2*, 219–227.
- (54) Bhattacharyya, K. Solvation dynamics and proton transfer in supramolecular assemblies. *Acc. Chem. Res.* **2003**, *36*, 95–101.
- (55) Ghosh, S.; Chattoraj, S.; Bhattacharyya, K. Solvation dynamics and intermittent oscillation of cell membrane: live Chinese hamster ovary cell. *J. Phys. Chem. B* **2014**, *118*, 2949–2956.
- (56) Sasmal, D. K.; Ghosh, S.; Das, A. K.; Bhattacharyya, K. Solvation dynamic of biological water in a single live cell under a confocal microscope. *Langmuir* **2013**, *29*, 2289–2298.
- (57) Zimmer, C.; Wahnert, U. Nonintercalating DNA-binding ligands: specificity of the interaction and their use as tools in biophysical, biochemical and biological investigations of the genetic material. *Prog. Biophys. Mol. Biol.* **1986**, *47*, 31–112.
- (58) Dann, O.; Bergen, G.; Demant, E.; Volz, G. Trypanocide diamidines of 2-phenylbenzofuran, 2-phenylindene and 2-phenyl-indole. *Justus Liebigs Ann. Chem.* **1971**, *749*, 68–89.
- (59) Chiang, S. Y.; Welch, J.; Rauscher, F. J., III; Beerman, T. A. Effects of minor groove binding drugs on the interaction of TATA box binding protein and TFIIA with DNA. *Biochemistry* **1994**, *33*, 7033–7040.
- (60) Welch, J. J.; Rauscher, F. J., III; Beerman, T. A. Targeting DNA-binding drugs to sequence-specific transcription factor/DNA complexes. Differential effects of intercalating and minor groove binding drugs. *J. Biol. Chem.* **1994**, *269*, 31051–31058.
- (61) Bardhan, R.; Lal, S.; Joshi, A.; Halas, N. J. Theranostic nanoshells: from probe design to imaging and treatment of cancer. *Acc. Chem. Res.* **2011**, *44*, 936–946.
- (62) Szabo, A. G.; Krajcik, D. T.; Cavatorta, P.; Masotti, L.; Barcellona, M. L. Excited State pK_a behaviour of DAPI. A rationalization of the fluorescence enhancement of DAPI in DAPI-nucleic acid complexes. *Photochem. Photobiol.* **1986**, *44*, 143.
- (63) Liepinsh, E.; Leupin, W.; Otting, G. Hydration of DNA in aqueous solution: NMR evidence for a kinetic destabilization of the minor groove hydration of d-(TTAA)₂ versus d-(AATT)₂ segments. *Nucleic Acids Res.* **1994**, *22*, 2249–2254.
- (64) Mack, D. R.; Chiu, T. K.; Dickerson, R. E. Intrinsic bending and deformability at the T-A step of CCTTTAAAGG: A comparative analysis of T-A and A-T steps within A-tracts. *J. Mol. Biol.* **2001**, *312*, 1037–1049.
- (65) Fujii, S.; Kono, H.; Takenaka, S.; Go, N.; Sarai, A. Sequence-dependent DNA deformability studied using molecular dynamics simulations. *Nucleic Acid. Res.* **2007**, *35*, 6063–6074.
- (66) Nakagawa, H.; Yonetani, Y.; Nakajima, K.; Ohira-Kawamura, S.; Kikuchi, T.; Inamura, Y.; Kataoka, M.; Kono, H. Local dynamics coupled to hydration water determines DNA-sequence-dependent deformability. *Phys. Rev. E* **2014**, *90*, 022723–11.
- (67) Tataurov, A. V.; You, Y.; Owczarzy, R. Predicting ultraviolet spectrum of single stranded and double stranded deoxyribonucleic acids. *Biophys. Chem.* **2008**, *133*, 66–70.
- (68) DNA Thermodynamics & Hybridization. <http://biophysics.idtdna.com>.
- (69) Mazzini, A.; Cavatorta, P.; Iori, M.; Favilla, R.; Sartor, G. The binding of 4',6-diamidino-2-phenylindole to bovine serum albumin. *Biophys. Chem.* **1992**, *42*, 101–109.
- (70) Sen, S.; Andreatta, D.; Ponomarev, S. Y.; Beveridge, D. L.; Berg, M. A. Dynamics of water and ions near DNA: comparison of simulation to time-resolved stokes-shift experiments. *J. Am. Chem. Soc.* **2009**, *131*, 1724–1735.
- (71) Pal, S.; Maiti, P. K.; Bagchi, B.; Hynes, J. T. Multiple time scales in solvation dynamics of DNA in aqueous solution: the role of water, counterions, and cross-correlations. *J. Phys. Chem. B* **2006**, *110*, 26396–26402.
- (72) Furse, K. E.; Corcelli, S. A. The dynamics of water at DNA interface: computational study of Hoechst-33258 bound to DNA. *J. Am. Chem. Soc.* **2008**, *130*, 13103–13109.
- (73) Furse, K. E.; Corcelli, S. A. Molecular dynamics simulations of DNA solvation dynamics. *J. Phys. Chem. Lett.* **2010**, *1*, 1813–1820.
- (74) Furse, K. E.; Corcelli, S. A. Dynamic signature of abasic damage in DNA. *J. Am. Chem. Soc.* **2011**, *133*, 720–723.
- (75) Bagchi, B. Anomalous power law decay in solvation dynamics of DNA: a mode coupling theory analysis of ion contribution. *Mol. Phys.* **2014**, *112*, 1–9.
- (76) Johannesson, H.; Halle, B. Minor groove hydration of DNA in solution: dependence on base composition and sequence. *J. Am. Chem. Soc.* **1998**, *120*, 6859–6870. Mcateer, K.; Ellis, P. D.; Kennedy, M. A. The effects of sequence context on base dynamics at TpA steps in DNA studied by NMR. *Nucleic Acid Res.* **1995**, *23*, 3962–3966.
- (77) Mcateer, K.; Ellis, P. D.; Kennedy, M. A. The effects of sequence context on base dynamics at TpA steps in DNA studied by NMR. *Nucleic Acid Res.* **1995**, *23*, 3962–3966.